ASTRONOMY
AND
ASTROPHYSICS

Pumping of Class II methanol masers

II. The $5_1-6_0\,A^+$ transition

A.M. Sobolev[1], D.M. Cragg[2], and P.D. Godfrey[2]

[1] Astronomical Observatory, Ural State University, Lenin Street 51, Ekaterinburg 620083, Russia (Andrej.Sobolev@usu.ru)

[2] Department of Chemistry, Monash University, Clayton, Victoria 3168, Australia (Dinah.Cragg@sci.monash.edu.au and Peter.Godfrey@sci.monash.edu.au)

Abstract. We present large velocity gradient (LVG) model calculations which explain the observed intensities ($> 10^{12}$ K) of the $5_1-6_0\,A^+$ methanol line at 6 GHz, which is the brightest of the strong Class II methanol masers. Our model of radiative transfer in the maser source was described in the first paper of this series devoted to the excitation of the $2_0-3_{-1}\,E$ transition at 12 GHz (Sobolev & Deguchi, 1994a, Paper I). We consider several collisional models for A-species methanol. Line overlap is found to have little effect on the intensities of the brightest methanol maser lines.

The present calculations confirm that pumping operating through the levels of the second and first torsionally excited states can explain the existence of masers, and the observed brightnesses of the $5_1-6_0\,A^+$ and $2_0-3_{-1}\,E$ lines in W3(OH). The pumping mechanism requires ambient dust of temperature > 150 K with the maser regions having methanol column densities $> 2\cdot10^{15}$ cm^{-2} and hydrogen number densities $< 10^8$ cm^{-3}. The strongest masers present in the vicinity of H II regions should be beamed. We find that the required methanol abundance is such that conditions in Class II methanol masers are likely to be influenced by the passage of shock waves. Recently discovered variability in the strongest methanol maser lines could be explained by movements of the medium.

The brightness of the $5_1-6_0\,A^+$ methanol line in our model is strongly determined by the free-free radio continuum emission from the underlying ultracompact H II region. This emission strongly influences the excitation of the saturated $5_1-6_0\,A^+$ transition, as well as providing a source of background radiation for amplification. It is shown that to produce the observed intensities of the strongest Class II methanol maser lines in W3(OH) the H II region emission should be highly diluted ($W_{\mathrm{HII}} < 3\cdot10^{-4}$). This implies that a substantial portion of the maser radiation forms in regions which are situated at a considerable distance from the H II region. Therefore, the conditions necessary for the appearance of masers with an underlying continuum source are likely to be produced by the shock wave preceding the ion-

ization front which forms the ultracompact H II region. It is shown that Class II maser spots most probably correspond to radial velocity correlation paths in the turbulent medium. This example shows how the combined observation of 6 and 12 GHz methanol masers can be used to delimit physical conditions in star-forming regions.

1. Introduction

The $5_1-6_0\,A^+$ methanol line at 6 GHz is the brightest of the strong Class II methanol masers. Detection of widespread emission in this line was first reported by Menten (1991). At present extensive surveys have yielded about three hundred 6 GHz maser sites (see Caswell 1996 for references and new detections). Class II methanol masers are always found in regions of recent massive star formation and many of them are associated with known ultracompact H II regions. The widespread occurrence and high intensity of the $5_1-6_0\,A^+$ line makes it one of the best tracers of star-forming regions at present.

Interferometric studies indicate that the $5_1-6_0\,A^+$ line is extremely bright. For example, the brightness temperature in a number of maser spots in the prototypic Class II maser source, W3(OH), is $3\cdot10^{12}$ K and higher (Menten et al. 1992). Such a high value provides a strong constraint on the excitation mechanism. The other major constraint comes from the observed ratio of brightnesses of spatially coincident (Menten et al. 1992; Norris et al. 1993) maser sources in the 6 GHz $5_1-6_0\,A^+$ and 12 GHz $2_0-3_{-1}\,E$ lines. For a sample of 131 $2_0-3_{-1}\,E$ maser sources, Caswell et al. (1995b) found that the 6 GHz to 12 GHz intensity ratio ranges from 0.39 to 85, with a median value of 3.2. For their sample of stronger 6 GHz masers, a median value of 26 was found for this ratio. So, 12 GHz features are typically weaker than their 6 GHz counterparts, though there are some

Send offprint requests to: D.M. Cragg

sites where they are stronger (Caswell et al. 1995b,c), including NGC 6334F (Ellingsen et al. 1996a). In W3(OH) the peak 12 GHz brightness is approximately $2 \cdot 10^{10}$ K (Menten et al. 1988), so that the 6 GHz line is approximately 150 times brighter.

In the first papers dedicated to quantitative explanation of Class II methanol maser characteristics, it was shown that the phenomenon appears only when the brightness temperature of the external radiation is greater than the kinetic temperature in the source itself (Cragg et al. 1992, Zeng 1992, Peng & Whiteoak 1993a). However, these pioneering models failed to produce bright enough masers.

In the paper of Sobolev & Deguchi (1994a, Paper I) it was shown that the brightness temperatures of the 12 GHz $2_0 - 3_{-1} E$ line could be explained in a more elaborate model taking into account maser beaming and involving energy levels of torsionally excited states. Brightness was strongly influenced by background radiation of the ultracompact H II region. In Paper I the model was applied only to the E symmetry species of methanol. In the current work, the same model is applied to A-species methanol in order to investigate the 6 GHz $5_1 - 6_0 A^+$ line. Some details of the model are briefly described in the following section. It is noteworthy that the model naturally explains the recently found variability of the $2_0 - 3_{-1} E$ (Caswell et al. 1993) and $5_1 - 6_0 A^+$ (Caswell et al. 1995a) brightness by changes of geometry of the beamed maser source.

The current study is devoted to the main problems of Class II methanol maser modelling: explanation of the $5_1 - 6_0 A^+$ line brightness and the 6 GHz to 12 GHz brightness ratio. Special attention is paid to the brightness ratio and what one can deduce from its value, because these two lines are the only widespread manifestations of Class II maser activity.

2. Description of the model

Our model for pumping the 6 GHz $5_1 - 6_0 A^+$ transition of interstellar methanol is the same as that presented in Paper I for the 12 GHz $2_0 - 3_{-1} E$ transition. The masers are assumed to arise in portions of methanol-rich gas within a spherically expanding cloud and can be beamed. (In the large velocity gradient model beaming is expressed by $\varepsilon^{-1} = \tau_0/\tau_\perp = d(\ln r)/d(\ln V)$ in definitions of Castor (1970). We treat LVG as a convenient approximation for studying the vast parameter space and think that actual beaming mainly comes from the maser source geometry). When the masers lie along the line of sight to an H II region it provides a source of background radiation for amplification by the maser lines, in the tail of the free-free continuum spectrum. The actual maser pumping is done by warm dust which surrounds the methanol-rich portions of matter, providing an infrared continuum source to pump the first and second torsionally excited states of methanol. Dust with the necessary properties is known to be present in the vicinity of ultracompact H II regions (see Walmsley 1995 for a recent review, and Wink et al. 1994 for recent W3(OH) observational data). Model equations are given in the Appendix.

Actually, the torsionally excited states play the role of transmitters of population between the levels of the ground state

which form the maser transition. Although the details of operation of the pumping mechanism are quite complicated (see Sobolev & Deguchi 1994b) in Paper I it was shown that the most prominent pump cycles have similar characteristics. They are: excitation to a level of the 2nd torsionally excited state followed by spontaneous decay through the levels of the 1st torsionally excited state to the levels of the ground state. Radiative rates for methanol are such that spontaneous decay favours downward transitions to levels of the ground state with K quantum number different from that of the initial state. This is the pattern which causes the appearance of masers.

It is worth mentioning that the Rosseland theorem, which works in the presence of diluted black-body radiation, can be applied to this pumping mechanism. This theorem was proved for the case of dilution factors $W < 1$ by Sobolev et al. (1985) and can be relatively easy proved for the case when the external radiation field is determined by emission of dust with finite optical depth using a thermodynamic approach from the above paper. The theorem states that radiative processes lead to splitting of higher energy photons into sets of photons with lower energy. The efficiency of this process is greatest when the higher energy photon splits into photons with equal energy. This causes a much higher efficiency of pumping through the levels of the 2nd torsionally excited state than can be obtained by pumping through the 1st torsionally excited levels, as demonstrated in Paper I.

Symmetry considerations allow two distinct species of methanol, conventionally labelled A and E. Methanol molecules of one symmetry species cannot be converted at significant rates into the other by the normal interstellar radiative and collisional excitation processes; rather, the partitioning between the two species is determined during the chemical formation of methanol. Excitation modelling therefore treats the two species quite independently, although they must of course coexist under the same conditions, and with approximately equal abundance (depending on the temperature of formation). Here we model both species, since we are interested in comparing the $5_1 - 6_0 A^+$ and $2_0 - 3_{-1} E$ transitions.

Methanol energy levels up to rotational quantum number $J = 12$ and torsional quantum number $v_t = 2$ were calculated according to De Lucia et al. (1989), and Einstein coefficients for radiative transitions within and between the torsional levels were taken from Cragg et al. (1993). As described in Paper I, the number of ground state levels included is determined mainly by the kinetic temperature, and the corresponding levels in the torsionally excited states were included also. In the majority of calculations described in this paper, there were 279 levels of A-species methanol (93 in each torsional state), and 282 levels of E-species methanol (94 in each torsional state).

The details of excitation of methanol in collisions with hydrogen and helium are unfortunately unknown. Here we adopt the collision model of Peng & Whiteoak (1993b), based on double resonance experiments on E-species methanol by Lees & Haque (1974). There are some differences in the numerical results reported here for the 12 GHz $2_0 - 3_{-1} E$ transition from those reported in Paper I, due to an error in implementing the

collision model, which has now been corrected. We use the same propensity rules for the A-species, although there are no corresponding experimental results. As in Paper I, collisional transitions were included only between levels of the torsional ground state. For the A-species the rate of $\Delta J = 0$, $\Delta |K| = 0$ asymmetry doublet transitions also must be specified. We set Peng & Whiteoak's $f-$factor to unity for these transitions, but we also report some calculations where these transitions were forbidden altogether. In addition, we examine the effects of non-selective collisions.

An examination of the role of numerous line overlaps has shown that they produce a negligible effect on the $5_1-6_0 A^+$ line intensity, and so we do not consider them further in the present paper. We plan to describe the overlap effects in a subsequent paper on the other methanol masering transitions, some of which are enhanced by overlap.

3. Variation of parameters

In this paper we investigate whether the model of Paper I which successfully accounted for the brightness of the strongest observed $2_0-3_{-1} E$ methanol masers can also account for the $5_1-6_0 A^+$ observations. We begin with the model conditions which gave peak brightness for the 12 GHz $2_0-3_{-1} E$ line (model D2 of Paper I), then explore the parameter space by varying certain of the model conditions, singly and in combination. Several hundred runs were done for each species. We present the results in terms of the brightness of the 6 GHz $5_1-6_0 A^+$ line, T_6, and the brightness temperature ratio of the 6 GHz to 12 GHz lines, $R_{6,12} = T_6/T_{12}$. Generally speaking the 6 GHz and 12 GHz transitions become inverted under the same conditions in our model, and the 6 GHz maser is brighter, as is usually observed.

Our standard model has the following parameters: molecular hydrogen density $n_H = 10^{7.5}\, cm^{-3}$, gas kinetic temperature $T_{kin} = 30\, K$, dust continuum temperature $T_d = 175\, K$, beaming parameter $\varepsilon^{-1} = 10$, dust filling factor $W_d = 0.5$, dust optical depth at 10^{13} Hz $\tau_{13} = 1$, H II region dilution factor $W_{HII} = 2\cdot10^{-3}$, and methanol specific column density $N_M/\Delta V = 1.5\cdot10^{12}\, cm^{-3}\, s$. The last quantity corresponds to the methanol column density divided by line width, or equivalently to the methanol abundance divided by velocity gradient. Usually this quantity is considered in terms of the methanol fractional abundance X and velocity gradient dV/dr. The cited value appears, for example, with $X = 10^{-5}$ and $dV/dr = 6168\, km\, s^{-1}\, pc^{-1}$. Such velocity gradient corresponds to a line width $\Delta V = 0.1\, km\, s^{-1}$ over a maser dimension of $5\cdot10^{13}\, cm$.

These standard parameters are equivalent to the D2 model described in Paper I. With the collision model of Peng & Whiteoak (1993b) we find the brightness temperature of the 6 GHz maser to be $T_6 = 1.4\cdot10^{11}\, K$, while the brightness of the 12 GHz maser becomes $T_{12} = 5.4\cdot10^{10}\, K$, and so the ratio is $R_{6,12} = 2.7$. This degree of maser brightness is sufficient to account for the observations of the 12 GHz maser in W3(OH) (Menten et al. 1988), but not the 6 GHz maser (Menten et al. 1992). By varying the parameters of the model we seek

conditions under which T_6 approaches $3\cdot10^{12}$ K while T_{12} remains of order $2\cdot10^{10}$ K so that $R_{6,12} \simeq 150$ in order to model W3(OH). The data can also be used to deduce conditions in other sources for which observations of both lines are available. Indeed, the standard model represents saturated masing, and the ratio $R_{6,12} = 2.7$ is close to the median observed value of 3.2 (Caswell et al. 1995b).

Fig. 1 shows the effects on T_6 and $R_{6,12}$ of varying certain of the model parameters one at a time about the standard conditions. W_d and τ_{13} are fixed at the standard values in all runs.

It is apparent from Fig. 1a that the brightness ratio $R_{6,12}$ can be substantially increased by reducing the hydrogen density n_H to approximately $10^6\, cm^{-3}$. We would like to note here that reduction of n_H with a fixed value of X leads to a corresponding reduction of the specific column density which is actually responsible for the increase in $R_{6,12}$. This happens because the brightness of the 6 GHz line begins to increase at a lower value of column density than for the 12 GHz line. The ratio $R_{6,12}$ is not particularly sensitive to the other model parameters (Fig. 1 b-f), and remains > 1 so long as the beaming parameter $\varepsilon^{-1} > 3$. However, reducing n_H from its initial value of $10^{7.5}$ to 10^6 brings the 6 GHz $5_1-6_0 A^+$ brightness temperature T_6 down by two orders of magnitude (Fig. 1a), far below the W3(OH) observations. The graph suggests that only a reduction of W_{HII} can substantially enhance T_6 in compensation (Fig. 1f). Thus the combined 6 and 12 GHz observations in W3(OH) define a maser regime both further away from the H II region and of more moderate column density than was initially assumed. These considerations are borne out by further calculations, described below, but first the individual model parameters are discussed.

Fig. 1a displays the effect of varying the hydrogen number density n_H, while keeping the methanol fractional abundance fixed at $X = 10^{-5}$. Both T_6 and T_{12} peak at $n_H = 10^{7.5}\, cm^{-3}$, which is our standard model. At higher hydrogen densities both transitions switch over to absorption as the effects of collisions become more dominant. At lower densities $R_{6,12}$ increases to a maximum of 89 at $n_H = 10^{6.2}\, cm^{-3}$, but T_6 is only $1.3\cdot10^9$ K at this density. So reducing the density with a fixed value of fractional abundance produces an increased brightness ratio, but greatly diminishes the actual brightness of both masers.

Although Fig. 1 displays the effects of varying other model parameters only at fixed hydrogen density $n_H = 10^{7.5}\, cm^{-3}$, calculations were also done over the range of densities $10^5 - 10^8\, cm^{-3}$. We found it very helpful to consider the dependence of maser characteristics on hydrogen density when plotted as a function of specific column density. This comes from the fact that in the definition of optical depth the specific column density represents a factor containing all physical parameters of the source apart from the excitational pattern. The brightness of masers has exponential dependence on the value of optical depth and much weaker linear dependence on the value of source function. For the strong masers this difference is very greatly pronounced. Hence, for the current study the scale is almost completely determined by the value of specific column density. This is illustrated in Fig. 2, showing the dependence of
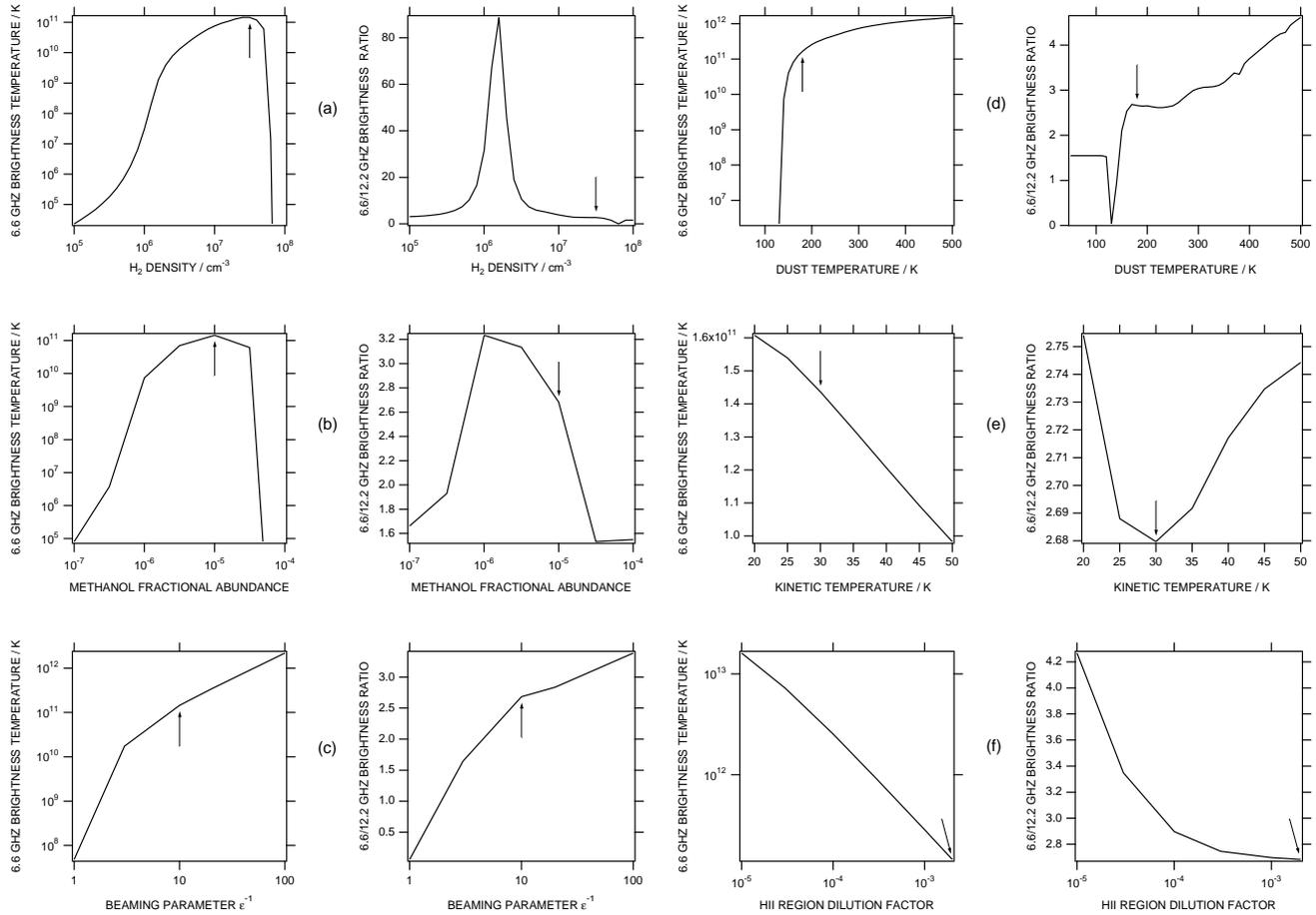
Fig. 1a–f. Effects of varying the model parameters one-at-a-time from the D2 standard conditions of Paper I on the 6 GHz brightness T_6 and the 6 GHz to 12 GHz brightness ratio $R_{6,12}$. The position of the standard model is marked with an arrow in each case.

the brightness temperature T_6 and ratio $R_{6,12}$ on specific column density for different values of hydrogen number density. Elsewhere in this paper we use the more traditional set of parameters including n_H and X.

Fig. 2a illustrates the fact that when densities are lower than 10^8 cm^{-3} the curve for T_6 remains almost invariant: exponential growth until the negative optical depth reaches approximately 11 (this value is determined mainly by W_{HII}), and subsequent gradual saturation which prevents T_6 from exceeding some upper limit. For the models shown on the plot saturation begins at specific column densities about 10^{11} cm^{-2}s. At this point we merely want to show that T_6 cannot be infinitely increased. The dependence of the upper limit on the remaining parameters will be discussed further. It should be noted that the curve for $n_H = 10^8$ cm^{-3} reaches substantially lower peak brightness than the others. This indicates that the methanol maser sources are not likely to have such high densities.

Fig. 2b shows that there is a narrow specific column density window ($10^{10.4} - 10^{11.6}$ cm^{-2}s for $\varepsilon^{-1} = 10$) in which the 6 GHz maser is brighter than the 12 GHz maser by 1 to 2 orders of magnitude. This contrasts with the modest ratios ($R_{6,12}$ about 3) found at other column densities, irrespective of other

model parameters. As was noted above this comes about because the 6 GHz maser switches on at a lower column density than the 12 GHz maser. Fig. 2b shows that the peak value of $R_{6,12}$ grows with decreasing number density, while its position shifts to slightly higher specific column density. This may be used as a guideline in searching for bright models with high values of $R_{6,12}$. However, if the maser source is an isolated clump, hydrogen number densities in bright maser sources ($T_6 > 10^9$ K) cannot be lower than 10^6 cm^{-3} without violating the upper limits on methanol fractional abundance ($< 10^{-5}$) and source size ($5 \cdot 10^{13}$ cm for the observed maser spots) under the assumption of plausible values for line width.

The methanol fractional abundance X was varied over the range $10^{-7} - 10^{-4}$ (assuming $dV/dr = 6168$ km s^{-1} pc^{-1}). As shown in Fig. 3, increasing the fractional abundance produces the 6 GHz maser brightness peak at progressively lower density, but the peak in the brightness ratio also shifts to a correspondingly lower density. Thus changes in X alone are not sufficient to give simultaneous high values of T_6 and $R_{6,12}$. Neither maser increased significantly in peak brightness at abundances beyond our standard value of $X = 10^{-5}$, showing the effects of saturation. This exceptionally high level of methanol abundance is
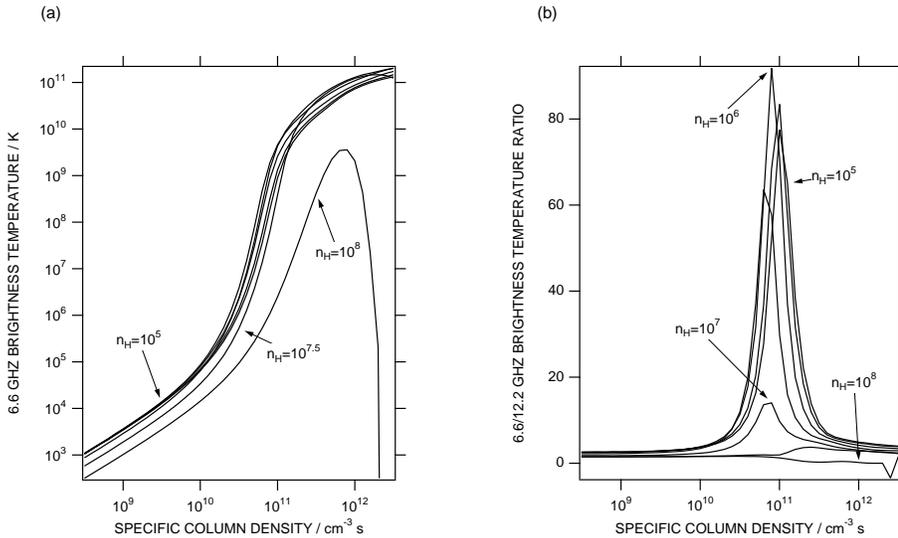
Fig. 2a and b. Effects of varying the hydrogen density n_H and methanol specific column density $N_M/\Delta V$ on **a** the 6 GHz brightness T_6 **b** the 6 GHz to 12 GHz brightness ratio $R_{6,12}$. n_H takes the values $10^5, 3 \cdot 10^5, 10^6, 3 \cdot 10^6, 10^7, 3 \cdot 10^7, 10^8 \, cm^{-3}$ on successive curves.

required to explain the observed W3(OH) maser brightness, and is discussed further in the next section.

In the majority of calculations reported here, we assume the abundance of both symmetry species to be equal, $[A] = [E]$. The combined statistical weight of the A-species ($A1 + A2$ in the $C_{3v}(M)$ molecular symmetry group) is balanced by the double torsional degeneracy of the E-species ($E1 + E2$ in the notation of Lees 1973). However, because the ground state energies of the two species differ by $5.49 \, cm^{-1}$, if the chemical equilibrium between the two species was set at low temperature, the A-species will be slightly more abundant. If we assume that the high methanol abundance in the maser regions is a result of evaporation from grain mantles, where the methanol may have been formed at temperatures as low as 10 K, then the abundance ratio between the two symmetry species becomes $[A]/[E] = 1.44$. Under our standard model conditions if we increase column density by a factor of 1.44 for the A-species only, we find that T_6 is not significantly altered; however there is more effect at low density, and $R_{6,12}$ increases to 469 at $n_H = 10^6 \, cm^{-3}$.

Fig. 1c shows the effects of varying the beaming parameter ε^{-1} from 1 to 100. We conclude that $\varepsilon^{-1} > 3$ is required to account adequately for the brightest 6 and 12 GHz methanol masers $> 10^{10}$ K. Greater values of beaming were included to seek simultaneous high values of T_6 and $R_{6,12}$. Although greater beaming increases the peak value of T_6, it also shifts the peak $R_{6,12}$ value to lower density, as shown in Fig. 4. Thus greater beaming, like greater methanol fractional abundance, can generate brighter masers at a lower hydrogen density, but not the high values of the ratio also required for W3(OH). In contrast, the 12 GHz maser is brighter than the 6 GHz maser ($R_{6,12} < 1$) when $\varepsilon = 1$ and $n_H > 10^7 \, cm^{-3}$, suggesting that observations of $R_{6,12} < 1$ in some sources are indicative of a different maser geometry.

Fig. 1d shows the effects of varying the dust temperature T_d between 50 and 500 K. There is a steep rise in maser brightness when T_d approachs 150 K, i.e., when the maximum of the dust

emission is shifted to the values of frequency corresponding to transitions between the ground and the second torsionally excited state. At $T_d > 150$ K these transitions prevail and the masers (pumped by the dust continuum radiation) become less sensitive to the dust temperature. At lower gas densities there is even less variation. For $T_d > 200$ K, T_6 exceeds 10^{12} K at $n_H = 10^8 \, cm^{-3}$, and T_{12} exceeds $5 \cdot 10^{11}$ K. This 12 GHz brightness is larger than that observed in W3(OH), suggesting that the dust temperature is probably not this high. Our results with $T_d > 200$ K should be treated with some caution, since the number of energy levels included in our calculations may be inadequate here (levels of the third torsionally excited state and those of vibrationally excited states are not included).

The major source of uncertainty in excitation modelling of methanol is the collisional excitation rates, which as discussed earlier are based on propensity rules derived from a few experiments on the E-species alone. We therefore tried as an alternative a model involving nonselective collisions (Goldreich & Kwan 1974). The total collision cross section was chosen to be the same as that given by the model of Peng & Whiteoak. We compared the two models over the density range $n_H = 10^5 - 10^8 \, cm^{-3}$, with other parameters as in our standard model. The major change was that the peak T_6 value at $n_H = 3 \cdot 10^7 \, cm^{-3}$ fell to $3.9 \cdot 10^{10}$ K, while $T_{12} = 3.5 \cdot 10^{10}$ K, so that the ratio $R_{6,12}$ was reduced to 1.1. At lower densities there was less variation in maser brightness, and the peak ratio was $R_{6,12} = 81$ at $n_H = 10^6 \, cm^{-3}$. We conclude from this that the pumping mechanism which generates the strongest Class II methanol masers in our model is not strongly dependent on the details of the collision model, but that the ratio of 6 to 12 GHz maser brightness temperatures is more sensitive to the choice of these rates. Thus it may not be possible to properly model the A-species masers until accurately calculated collisional excitation rates become available.

In addition, we looked at the effects of changing the kinetic temperature between 20 and 50 K within Peng & Whiteoak's collision model (Fig. 1e), and of forbidding collisional transi-
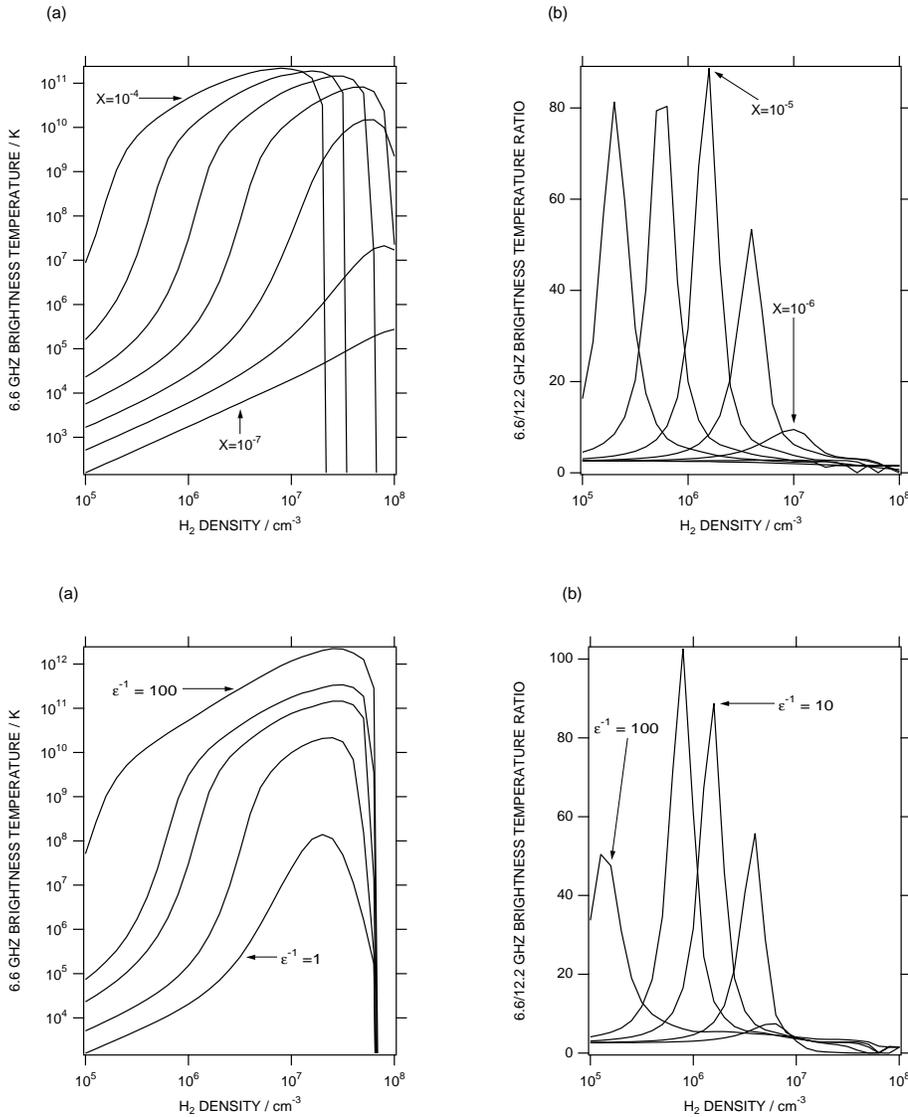
(a)

(b)

Fig. 3a and b. Effects of varying the methanol fractional abundance X and hydrogen density n_H on **a** the 6 GHz brightness T_6 **b** the 6 GHz to 12 GHz brightness ratio $R_{6,12}$. X takes the values $10^{-7}, 3 \cdot 10^{-6}, 10^{-6}, 3 \cdot 10^{-5}, 10^{-5}, 3 \cdot 10^{-4}, 10^{-4}$ on successive curves.

(a)

(b)

Fig. 4a and b. Effects of varying the beaming parameter ε^{-1} and hydrogen density n_H on **a** the 6 GHz brightness T_6 **b** the 6 GHz to 12 GHz brightness ratio $R_{6,12}$. ε^{-1} takes the values 1,3,10,20,100 on successive curves.

tions between asymmetry doublet levels in the A-species, but the changes in both cases were very minor. All these results are consistent with the idea that the Class II methanol masers are pumped by radiative processes, and collisional processes are not responsible for the generation of the strongest Class II masers, influencing only quantitative details. The gas-dust temperature difference may in fact be less than assumed, but it is not possible to adequately model rather dense gas with temperatures > 50 K with the current truncated set of energy levels. Moreover, additional calculations with a larger set of energy levels have shown that if masers are formed in low density regions, the gas can be even warmer than the surrounding dust.

In Fig. 5 we show the effects of varying the H II region dilution factor W_{HII} between our standard value of $2 \cdot 10^{-3}$ and 10^{-5}. We also investigated two limiting cases: one where the H II region is removed altogether from the model, and another where it becomes infinitely diluted. The maser brightness increases progressively as W_{HII} is reduced. This comes from the effect of saturation of the masering transition, which restricts the population inversion when the angle-averaged intensity in the maser line exceeds some threshold value. With lower values of W_{HII} this threshold is achieved at greater values of negative optical depth, which determines the brightness. Hence, reduction of W_{HII} permits higher values of T_6 through diminishing influence of saturation. On the other hand, the H II region provides a source of background radiation for amplification which is independent of the distance between the source and the maser. In our model the H II region is about 6300 times brighter than the 2.7 K microwave background and this makes possible to create the strongest masers. At densities below $10^{6.5}$ cm^{-3} both the 6 GHz brightness and $R_{6,12}$ become large as W_{HII} is reduced. This regime is the only set of model conditions found capable of accounting for the observations in W3(OH), under the assumption that the maser spot is an isolated clump. Thus for example when $W_{HII} = 10^{-5}$ and $n_H = 3 \cdot 10^6$ cm^{-3}, we find $T_6 = 1.3 \cdot 10^{12}$ K, $T_{12} = 1.5 \cdot 10^{10}$ K and $R_{6,12} = 91$. The ratio increases further as W_{HII} is further reduced.
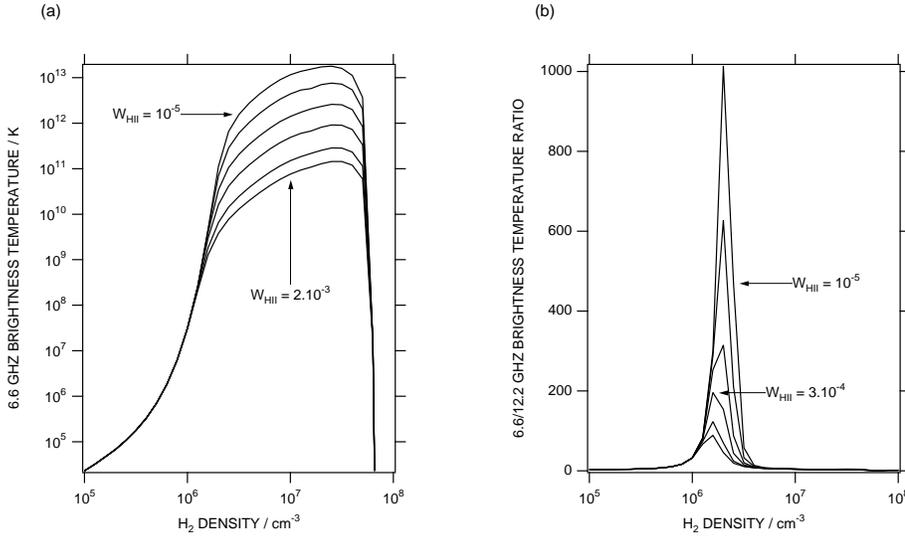
Fig. 5a and b. Effects of varying the H II region dilution factor W_{HII} and hydrogen density n_H on **a** the 6 GHz brightness T_6 **b** the 6 GHz to 12 GHz brightness ratio $R_{6,12}$. W_{HII} takes the values $2 \cdot 10^{-3}, 10^{-3}, 3 \cdot 10^{-4}, 10^{-4}, 3 \cdot 10^{-5}, 10^{-5}$ on successive curves.

Table 1. Selected model results for 6 and 12 GHz brightness temperatures (see text for definition of parameters). All models have $W_d = 0.5$, $\tau_{13} = 1$, $dV/dr = 6168 \, \text{km s}^{-1}\text{pc}^{-1}$, $X = 10^{-5}$, $T_d = 175 \, \text{K}$ and $T_{kin} = 30 \, \text{K}$.

	standard	low n_H	low W_{HII}	$[A] = 1.44[E]$	$\varepsilon = 1$
ε^{-1}	10	10	10	10	1
$n_H(\text{cm}^{-3})$	$10^{7.5}$	$10^{6.2}$	$3 \cdot 10^6$	$3 \cdot 10^6$	$10^{7.5}$
W_{HII}	$2 \cdot 10^{-3}$	$2 \cdot 10^{-3}$	10^{-5}	10^{-5}	$2 \cdot 10^{-3}$
$T_6(\text{K})$	$1.4 \cdot 10^{11}$	$1.3 \cdot 10^9$	$1.3 \cdot 10^{12}$	$3.0 \cdot 10^{12}$	$4.8 \cdot 10^7$
$T_{12}(\text{K})$	$5.4 \cdot 10^{10}$	$1.4 \cdot 10^7$	$1.5 \cdot 10^{10}$	$1.5 \cdot 10^{10}$	$8.0 \cdot 10^8$
$R_{6,12}$	2.7	89	91	206	0.06

Finally we have done calculations with reduced W_{HII} and [A]/[E] enhanced, in order to maximise the ratio $R_{6,12}$ while maintaining very high levels of maser brightness. Some representative results are summarized in Table 1.

4. Discussion

The results of the preceding section show that the model under consideration can explain the observed high brightnesses T_6 of the $5_1 - 6_0 \, A^+$ line. Combined observations of both the $5_1 - 6_0 \, A^+$ and $2_0 - 3_{-1} \, E$ lines constrain the physical parameters of the maser sources and their environment.

We realize that the results of this paper are subject to the uncertainties of modelling, and the list of physical processes influencing the pump efficiency is not complete in our study. For example, collisions with relatively hot electrons in preshock regions can provide additional excitation, i.e. increase the pump rate, etc. However, relevant modelling is impossible at present mainly because of the lack of data on transition probabilities, etc. Corresponding studies in basic molecular physics will greatly benefit the solution of this problem.

Anyhow, at present there is no known alternative to pumping through torsionally excited levels which can explain the observed high brightnesses of the strongest Class II methanol masers. This paper describes the basic features of that mechanism, which appear to have a general character independent of the quantitative details of the torsional pumping. For example, beaming increases the 6 and 12 GHz brightness temperatures, etc.

In order to account for the extremely high observed values of T_6, T_{12} and $R_{6,12}$ the masers governed by the described pumping mechanism should be beamed with the factor $\varepsilon^{-1} > 3$. Lower beaming leads to decreased maser brightness because of dispersal of the pumping energy over a wider angle. Further, the 6 GHz methanol masers are quenched at hydrogen densities $\geq 10^8 \, \text{cm}^{-3}$. At the same time there should exist a lower limit for hydrogen number density. This value could be obtained through the relation

$$n_H = (N_M/\Delta V) \cdot \Delta V \cdot X^{-1} \cdot R^{-1}$$

derived from the definition of specific column density. Here R is the source size in the tangential direction.

Satisfactory agreement with observations under the described pumping mechanism is obtained with values of $(N_M/\Delta V) > 1.6 \cdot 10^{11} \, \text{cm}^{-3}\text{s}$. Further, the relative abundance of methanol can not be greater than 10^{-5} and ΔV can not exceed the thermal breadth ($= 10^4 \, \text{cm s}^{-1}$). So, we arrive at the estimate of the lower limit for density

$$n_H > 1.6 \cdot 10^{20} \text{cm}^{-2}/R.$$

Estimates of the source sizes depend greatly on the geometrical model. Assuming that the tangential dimensions of maser sources are equal to the observed sizes of maser spots ($\sim 5 \cdot 10^{13}$ cm, Menten et al. 1992) one finds that the hydrogen number density should exceed $3 \cdot 10^6 \, \text{cm}^{-3}$. However, the actual lower limit is not so strict even in the case when maser sources are isolated clumps because the strongest methanol masers are saturated. So, observed sizes of maser spots correspond to the dimensions of the unsaturated core which is smaller than the maser source itself. Moreover, if the maser spots represent correlation paths

in a turbulent medium (see below) the source size can be comparable to that of the ultracompact H II region ($\sim 6 \cdot 10^{16}$ cm). Under this assumption the densities in those portions of matter which contribute to the maser spot appearance can be as low as $3 \cdot 10^3$ cm^{-3}.

In order to supply enough energy for pumping masers through the levels of torsionally excited states the ambient dust should be sufficiently warm. Observed values of T_6 are achieved with $T_{\text{dust}} > 150$ K. It should be noted that the field of maser radiation in the proposed model looks like a hedgehog. So, a reasonable amount of warm dust can account for the total flux of methanol masers.

The calculations show that for production of the strong masers the methanol abundance relative to molecular hydrogen should be high. The required values are up to 10^{-5} and could be realized within $10^4 - 10^5$ yr after evaporation of grain mantles (see, e.g., Millar et al. 1991; Hartquist et al. 1995). Observations indicate that the methanol relative abundance can reach sufficiently high values, at least in hot cores and shocked regions (e.g., Plambeck & Menten 1990; Sobolev 1993). Studies of Orion by Jacq et al. (1993) and Saito et al. (1994) have shown that the relative abundance of deuterated and main species methanol strongly supports the grain evaporation mechanism for methanol abundance enhancement against other chemical processes.

Two possible origins of methanol maser sources with such parameters have been discussed in the current literature.

The first, denoted as the 'clump' hypothesis, was explicitly described in Paper I. In this hypothesis the maser sources are isolated elongated clumps influenced by the passage of shock waves. Such clumps could be formed as a result of the interaction of the shock with the interstellar cloud (see, e.g., results of calculations by Bedogni & Woodward 1990; Stone & Norman 1992), or alternatively could be primordial clumps. It is noteworthy that the shock can align the clumps and lead to formation of somewhat organized structures.

In the clump hypothesis the tangential dimensions of clumps should correspond to the observed sizes of maser spots. Under the constraints of the described pumping mechanism this implies that the clumps should have high densities and should be substantially elongated in the radial direction.

The weak point of this hypothesis is the need for low gas temperature in clumps with high methanol abundance. Sobolev & Deguchi suggested that the masering clump can undergo some efficient cooling process after the evaporation of grain mantles. In dense clumps the time-scale of chemical evolution is greater than the time-scale of cooling (Charnley et al. 1995). An alternative possibility is that methanol in dense clumps can be sputtered through grain-grain collisions without substantial heating of the gas. Such collisions can be initiated by the penetration of grains accelerated by a shock propagating in the less dense ambient medium. Rough estimates show that a considerable portion of the accelerated particles should be trapped in the dense clump. So, general considerations find no obvious contradictions, but more elaborate examination is necessary.

The second hypothesis, a protostellar disc, was proposed by Norris et al. (1993). This hypothesis is based on the fact that in some cases the maser spots lie along lines of an arc. In the protostellar disc the maser sources could be represented by actual clumps and by regions with correlated velocities. The latter possibility depends on the relation between systemic and chaotic motions in the disc.

Densities in the discs are quite high, so the gas temperature must be low in order not to quench the masers. Note that the temperatures in such formations are strongly controlled by the central emitting source, and cooling after the passage of a shock wave is less efficient than in the 'clump' hypothesis. The other possibility is that the masers could arise when the star has evaporated the grain mantles but has not yet heated up the gas. However, estimating these time-scales is not so easy and further careful examination is necessary.

According to present knowledge the following hypothesis of Class II methanol maser formation in the disc looks more plausible. The source has developed outflow (e.g., bipolar outflow). In the region of interaction between the outflow and the disc exists a layer of warm dust providing infrared photons for pumping the masers. Dust particles accelerated in the outflow region penetrate into the disc and initiate grain-grain collisions which lead to sputtering of methanol from grain mantles without substantial heating of the gas (the situation is similar to that described above in discussion of the 'clump' hypothesis). The temperature in the bulk of the disc can be low (see, e.g., Andre & Montmerle 1994). So, the above situation corresponds to conditions under which Class II methanol masers are created by the pumping mechanism described in the current paper. It should be noted that the above scenario is based on rough estimates and thorough examination involving fluid dynamics calculations is necessary.

For the 6 GHz masers in W3(OH), observational data suggests that the possible protostellar discs are small. Since our pumping mechanism requires $n_H < 10^8$ cm^{-3} such formations are not likely to have sufficient column densities.

The third hypothesis concerning formation of masers in a turbulent medium appeared when the results of this paper were under consideration (Sobolev, Wallin & Watson 1997, in preparation). In this hypothesis maser spots are formed as a result of radial velocity correlation in different parts of the source which have favourable conditions for population inversion. In such masers the sizes of the maser spots are determined by the spectrum of scales for turbulent formations. Since quite a high fraction of matter on the line of sight can contribute to the appearance of the maser, densities can be as low as $3 \cdot 10^3$ cm^{-3}, while satisfying the relation between the lower limit of necessary values of specific column density and the source size. That substantially distinguishes the turbulent hypothesis from the others and eases up the explanation of the high $R_{6,12}$ value in W3(OH). It is worth mentioning that in the low density regime the requirement of relatively low gas temperature is no longer necessary. Hence, the necessary thermodynamic conditions are created more easily. Moreover, portions of matter contributing significantly to maser brightness (i.e., those closer to the ob-

server) may be situated quite far from the background ultracompact HII region. Such conditions are favourable for the pumping mechanism described in this paper. Further, additional calculations have shown that with lower densities the current pumping mechanism does not require a difference between the kinetic temperature in the source and the temperature of the pumping radiation. Such thermodynamical conditions are easier to create. Though substantial effort is necessary to prove the 'turbulent' nature of the strongest Class II methanol masers this hypothesis is very promising.

It is shown that the brightness of the 6 GHz $5_1-6_0 A^+$ methanol line is strongly influenced by background emission. Observations indicate that many sources have an underlying ultracompact H II region which is bright in free-free radio continuum. This fact is supported by results of Menten et al. (1992) and recent observations of Ellingsen et al. (1996b) which have shown that sources of strong maser emission in the 6 GHz line often correlate with the peaks of continuum emission at corresponding frequencies. However, we would like to note that in sources with only the 2.7 K microwave background, values of T_6 exceeding 10^{11} K could be achieved.

The reported calculations show that H II region emission strongly influences the excitation of the saturated $5_1-6_0 A^+$ transition, as well as providing a source of background radiation for amplification. To produce the ratio of intensities of the strongest Class II methanol maser lines observed in W3(OH) ($R_{6,12}$ about 150), the H II region emission should be highly diluted ($W_{HII} < 3 \cdot 10^{-4}$). This implies that a considerable portion of the maser radiation is formed in regions situated rather far from the H II region (at least in W3(OH)). Conditions in those methanol masers are likely to be produced by a shock wave propagating closer to the observer, e.g., the one preceding the ionization front which forms the ultracompact H II region. However, it should be noted that the W3(OH) ratio is considerably larger than that seen in other methanol maser sources (Caswell et al. 1995b). Such ratios could be realized in sources with less diluted background emission.

5. Conclusion

This work has confirmed that torsional pumping can account for the simultaneous occurrence of 6 and 12 GHz methanol masers, with the 6 GHz maser generally being brighter. The general conditions required for strong masers governed by this pumping mechanism have been defined: methanol rich ($X > 10^{-7}$) gas with moderate densities ($3 \cdot 10^3$ cm^{-3} < n$_H$ < 10^8 cm^{-3}), in the vicinity of warm dust ($T_d > 150$ K), with a beamed geometry ($\varepsilon^{-1} \geq 3$).

More specifically, an attempt has been made to use the observed maser ratio to delimit conditions in three different cases of Class II methanol maser formation with a strong continuum source in the background:

(1) The observations in W3(OH) ($R_{6,12} > 150$) and other strong 6 GHz sources (median $R_{6,12} = 26$) define a narrow column density regime where the 6 GHz maser turns on first, and highly diluted H II region emission for a prominent part of the

maser source. Possibly the $A-$species abundance is enhanced following evaporation of cold methanol from grains.

(2) In a 'typical' methanol maser source (median $R_{6,12} = 3.2$) the masers are likely to be greatly influenced by the effects of saturation.

(3) In sources where $R_{6,12} < 1$ such as NGC6334F the maser geometry involves less beaming and hydrogen density $> 10^7$ cm^{-3}.

These conclusions are subject to uncertainties of modelling, specifically in the collisional excitation rates and also in the nature of the sources and the treatment of radiative transfer. It is clear however that the existence of two strong and spatially coincident maser transitions in methanol provides a sensitive probe of the physical conditions in star formation regions.

Appendix A: model equations

The radiative transition probability for downward transitions is $A_{Ein} + B_{Ein} J_{av}$ where A_{Ein} and B_{Ein} are the Einstein coefficients for spontaneous and stimulated emission, and J_{av} is the mean integrated radiation field intensity at the line frequency. For the LVG model with expansion velocity $V(r)$ increasing with radius r according to $\varepsilon = d(\ln V)/d(\ln r) > 0$, then

$$
\begin{aligned}
J_{av} = \;& (1-\beta)B(T_x) + \beta B(T_{BB})\exp(-\tau_d) \\
& + W_d \beta B(T_d)(1 - \exp(-\tau_d)) \\
& + W_{HII}\beta_H(2h\nu^3/c^2)kT_{HII}/(h\nu)
\end{aligned}
$$

where $\beta = (1 - \exp(-\tau))/\tau$ is the escape probability for $\varepsilon = 1$, and for other values of ε, β is given as a function of τ by equation (A1) of Castor (1970).

Here the optical depth is

$$
\tau = (hc/(4\pi))(N/\Delta V)(n_{lo}/g_{lo} - n_{up}/g_{up})g_{up}B_{Ein}
$$

where n and g are the level populations and statistical weights respectively, N is the methanol column density and ΔV the velocity width of the source. The dust optical depth is $\tau_d = \tau_{13}(\nu/10^{13}$ Hz$)^2$ (the modeling is not greatly sensitive to the dust opacity law). The escape probability for the H II region is $\beta_H = (1 - \exp(-\tau_H))/\tau_H$, where $\tau_H = \tau/\varepsilon$, and the continuum emission intensity from the H II region is approximated by $(2h\nu^3/c^2)kT_{HII}/(h\nu)$. The Planck function is $B(T) = (2h\nu^3/c^2)[\exp(h\nu/(kT))-1]^{-1}$ where h is Planck's constant, ν is the line frequency, c is the speed of light and k is Boltzmann's constant. T_d is the dust temperature, W_d is the dust filling factor,

T_x is the line excitation temperature, and W_{HII} is the filling factor for the H II region. $T_{BB} = 2.7$ K is the cosmic background radiation temperature, and $T_{HII} = 18000 * [1 - \exp(-(12\,\text{GHz}/\nu)^2)]$, so for example $T_{HII} = 11183$ and 17294 K for the 12.178 GHz and 6.668 GHz lines, respectively.

The brightness temperature of the line above the continuum is

$$T_b = (h\nu/k)(1 - \exp(-\tau_H))\, exp(-\tau_d)[F(T_x)$$
$$- F(T_d)(1 - \exp(-\tau_d))$$
$$- F(T_{BB})\exp(-\tau_d) - kT_{HII}/(h\nu)]$$

where $F(T) = [\exp(h\nu/(kT)) - 1]^{-1}$.

References

Andre P., Montmerle T., 1994, A&A 420, 837

Bedogni R., Woodward P.R., 1990, A&A 231, 481

Castor J.I., 1970, MNRAS 149, 111

Caswell J.L., 1996, MNRAS 279, 79

Caswell J.L., Gardner F.F., Norris R.P. et al., 1993, MNRAS 260, 425

Caswell J.L., Vaile R.A., Ellingsen S.P., 1995a, Publ. Astron. Soc. Aust. 12, 37

Caswell J.L., Vaile R.A., Ellingsen S.P., Norris R.P., 1995b, MNRAS 274, 1126

Caswell J.L., Vaile R.A., Ellingsen S.P., Whiteoak J.B., Norris R.P., 1995c, MNRAS 272, 96

Charnley S.B., Kress M.E., Tielens A.G.G.M., Millar T.J., 1995, ApJ 448, 232.

Cragg D.M., Johns K.P., Godfrey P.D., Brown R.D., 1992, MNRAS 259, 203

Cragg D.M., Mekhtiev M.A., Bettens R.P.A., Godfrey P.D., Brown R.D., 1993, MNRAS 264, 769

DeLucia F.C., Herbst E., Anderson T., Helminger P., 1989, J.Molec.Spectrosc. 134, 395

Ellingsen S.P., Norris R.P., Diamond, P.J., et al. 1996a, In: King E.A. (ed.) Proceedings of Third Asia-Pacific Telescope Workshop. Australia Telescope National Facility, Sydney, p.106

Ellingsen S.P., Norris R.P., McCulloch P.M., 1996b, MNRAS 279, 101

Goldreich P., Kwan J. 1974, ApJ 189, 441.

Hartquist T.W., Menten K.M., Lepp S., Dalgarno A., 1995, MNRAS 272, 184

Jacq T., Walmsley C.M., Mauersberger R., et al., 1993, A&A 271, 276

Lees R.M., 1973, ApJ 184, 763

Lees R.M., Haque S.S., 1974, Can.J.Phys. 52, 2250

Menten K.M., 1991, ApJ 380, L75

Menten K.M., Reid M.J., Moran J.M., Wilson T.L., Johnston K.J., Batrla W., 1988, ApJ 333, L83

Menten K.M., Reid M.J., Pratap P., Moran J.M., Wilson T.L., 1992, ApJ 401, L39

Millar T.J., Herbst E., Charnley S.B., 1991, ApJ 369, 147

Norris R.P., Whiteoak J.B., Caswell J.L., Wieringa M.H., Gough R.G., 1993, ApJ 412, 222

Plambeck R.L., Menten K.M., 1990, ApJ 364, 555

Peng R.S., Whiteoak J.B., 1993a, Lect. Notes Phys. 412, 207

Peng R.S., Whiteoak J.B., 1993b, MNRAS 260, 529

Saito S., Mikami H., Yamamoto S., Murata Y., Kawabe R., 1994, in IAU Coll.140, Astronomy with Millimeter and Submillimeter Wave Interferometry, 241

Sobolev A.M., 1993, Lect. Notes Phys. 412, 219

Sobolev A.M., Deguchi S., 1994a, A&A 291, 569 (Paper I)

Sobolev A.M., Deguchi S., 1994b, ApJ 433, 719

Sobolev A.M., Strel'nitskii V.S., Chugai N.N., 1985, Astrofizika 22, 613, english translation: Astrophysics 22, 363

Sobolev A.M., Wallin B., Watson W.D., 1997, in preparation

Stone J.M., Norman.M., 1992, ApJ 390, L17

Walmsley M., 1995, Rev. Mex. Astron. Astrofis. (Serie de Conferencias) 1, 137

Wink J.E., Duvert G., Guilloteau S., Güsten R., Walmsley C.M., Wilson T.L., 1994, A&A 281, 505

Zeng Q., 1992, IAU Coll. 143, 341